Journal of Renewable Materials

Tech Science Press

DOI: 10.32604/jrm.2021.013816

ARTICLE

Function of Palm Fiber in Stabilization of Alluvial Clayey Soil in Yangtze River Estuary

Jili Qu* **and Hao Zhu***

Department of Civil Engineering, School of Environment and Architecture, University of Shanghai for Science and Technology, Shanghai, 200093, China

*Corresponding Authors: Jili Qu. Email: qujiliqwq@163.com; Hao Zhu. Email: Zhuhao2747@163.com

Received: 22 August 2020 Accepted: 12 November 2020

ABSTRACT

Palm fiber is one of the favorable materials used in stabilization of soft soil in geotechnical engineering projects in recent years due to its nature of sustainability, no harm to the environment, biodegradability, availability and cost-effectiveness in the context of widespread appeal from the world for returning to nature and protecting the earth our homestead. This paper is aimed at exploring the mechanical performance of Shanghai clayey soil reinforced with palm fiber. The unconfined compressive tests are carried out on samples treated with palm fibers of different lengths and contents, and the unconfined compressive strength (UCS), ductility rate (DR), secant modulus (SM), energy absorption capacity (EAC) and failure pattern (FP) of the reinforced and unreinforced samples have been analyzed with regard to their relationship with palm fiber contents and lengths. Then multiple regression, grey correlation and general correlation relationship analysis are applied to the resultant test data so as to obtain the mathematical and statistical equation of related soil indexes. It has been concluded from the analysis that the unconfined compressive strength, ductility and energy absorption capacity of reinforced soil will increase with the increase in content and length of palm fiber, which are maximized when palm fiber content and length are 0.4% and 15 mm, respectively. On the contrary, the secant modulus of reinforced soil decreases considerably with content and length of palm fiber as a whole. Additionally, the failure pattern also changes from brittle to ductile gradually with the content and length of palm fiber. The data provided by the analysis of reinforced soil can be referred to and used for the related geotechnical engineering in the future. And the mathematical model obtained from the statistical regression is significantly meaningful because it can be used to predict the soil performance without the need for doing the additional tests, with saving in cost and time. What's more, the application of palm fiber to soft soil is completely in accordance to the concept of sustainable development and environment protection.

KEYWORDS

Palm fiber; Shanghai clayey soil; UCS; EAC; multiple regression analysis

1 Introduction

Palm fiber is a common type of natural vegetable fiber material that had been widely used in many sectors in ancient society because of its high tensile property, ease of accessibility and environmental friendliness. For example, it had been commonly used for making all types of ropes, horse collars, saddles, and the likes in ancient Chinese society. With the persistent importance of the concept for

sustainable and green development, returning to natural world, palm fiber has been discovered its new uses in soil stabilization in recent decades: reinforcement material. Buildings, constructions and infrastructures on weak or soft soil are highly risky on geo-technical grounds because such soil is characterized by differential settlements, poor shear strength and high compressibility [1]. Therefore, the improvement of the soft soil has become indispensable before beginning a project. Traditional materials used for soil improvement, such as lime and cement as well as chemical stabilization, have gradually showed their weaknesses in the face of the control on climate change and environmental protection. For example, the production itself of 1 ton of cement and lime will averagely release 1 and 1.2 tons of CO_2, respectively, which affects negatively the climate change, while the emission of CO_2 from only manufacturing cement globally will account for 7–8% of total CO_2 emission [2]. In addition, many comparative materials have been used for soil stabilization, such as polypropylene fiber [3], construction waste [4], fly ash [5], solid waste [6], volcanic ash [7], concrete aggregate [8], etc.

Sajal et al. studied the effect of coir on the strength of soft soil, and confirmed the efficacy of using coir as a natural fiber to improve the soil strength characteristics [9]. The jute [10], linen fiber [11], specific vegetable fibers [12], have all been recently applied to soft soil to study the strength performance of treated samples, and they all show the reinforced effects to some degree. Momoh and Osofero reviewed the application of oil palm fibers to cement composites. They considered that are a lot of advantages for oil palm fiber to be used in stabilization of soil compared to traditional unsustainable materials such as lime, cement, etc. [13]. Very recently, the interface bond behavior of Glass Fiber-Reinforced Polymer (GFRP) tendons embedded in cemented soils has been investigated by pullout tests and unconfined compression tests, which shows close relationships between the ultimate bond strength of the GFRP tendons and the compressive strength of the cemented soils [14]. The behaviors of cement-treated marine clay [15], mechanical properties and durability of coal gangue reinforced cemented-soil mixture [16], freeze-thaw features of straw fiber-reinforced soil [17], and hydro-mechanical behavior of fiber reinforced dredged sludge [18] have been recently investigated, which show the enhanced effects on treated soils to some degree under different scenarios.

Because the oil palm fiber is of vegetable origin, it is readily available, considerably more economical to process and environmentally friendly. Use of sustainable materials such as palm fiber in the geotechnical engineering has been a predominant emphasis from engineers, researchers, practitioners, and scientists [19–25]. A lot of advantages of applying natural vegetable fibers to cementing composites have been presented in historical literature. Some of the impressive advantages include: Cost-effective, zero-carbon emission, light-weightiness, toughness, biodegradability, non-toxicity to the ecosystem and economic society, thermal insulation, enhanced acoustic insulation and strong recyclability [26–35]. Zahra et al. had been dedicating to study the plater mortars treated with palm fibers which showed an enhanced flexural and compressive strength [36]. Bushra et al. investigated the flexural, compressive and impact properties of sugar palm fibers (particle size 150 μm) reinforced phenolic composites, and the results showed that the mechanical properties of the composites are improved with the incorporation of fibers [37].

However, few researchers are focused on the effect of palm fibers on the strength features of clayey soil, which is extensively distributed across the middle and lower reaches of Yangtze river, China and frequently encountered in construction of civil engineering projects. Starting from the mouth of the Yangtze river, along the upper river west 500 km, the palm is widespread. Since 2000, about 120,000 palm plants have been introduced in Shanghai. By 2006, more than 320,000 palm plants had been planted in Shanghai [38]. It is expected according to the current increasing rate that there will be at least 1 million palm trees by 2030. According to statistics in 2010, the annual output of palm fiber was as many as 350,000 tons in China. And as an economic tree, the planting area of this tree shows an increasing trend year by year [39].

It also sees in some rural areas where rural housing and country-side highway are needed to construct on. Still, in recent years, the constructions in these areas are attaching significant weight to the sustainable and green development, which make the palm fiber a popular material for stabilizing the ground [40]. Natural palm fiber has excellent biodegradation resistance. After 3 months of soil burial, the mass loss rate was only 2.57%, showing its overwhelming superiority over flax fiber that has as high as 89.73% of mass loss if burial in soil for 3 months [41].

In view of its favorable features, this study will be focused on the researches on the effect of palm fibers from Chongming Island Shanghai China on the strength characteristics of Shanghai clayey soil. A series of unconfined compressive tests have been carried out on soil samples unreinforced and reinforced with palm fibers with different lengths and contents, and the unconfined compressive strength (UCS), ductility rate (DR), energy absorption capacity (EAC), secant modulus (SM) and failure pattern (FA) are measured and observed to diagrammatically analyze the role of palm fiber length and content on the UCS, DR, EAC, SM, FA. In addition, mathematical models are also established with statistical theory to further demonstrate their relations accurately and quantitatively, which would be more convenient and cost-effective in predicting their values without need for the labor or time of laboratory or field tests in future construction. Therefore, the present study is of great significance in construction of related areas, especially where sustainable and green developments are accorded top priority to.

2 Methods and Materials

2.1 Materials

2.1.1 Palm Fiber

The palm fiber has been obtained directly from the palm trees lining up on both side of Chenhai highway on Chongming island, Shanghai, China (Fig. 1). The basic physical, chemical, and mechanical characteristics of the palm fiber used in the test are shown in Tab. 1.

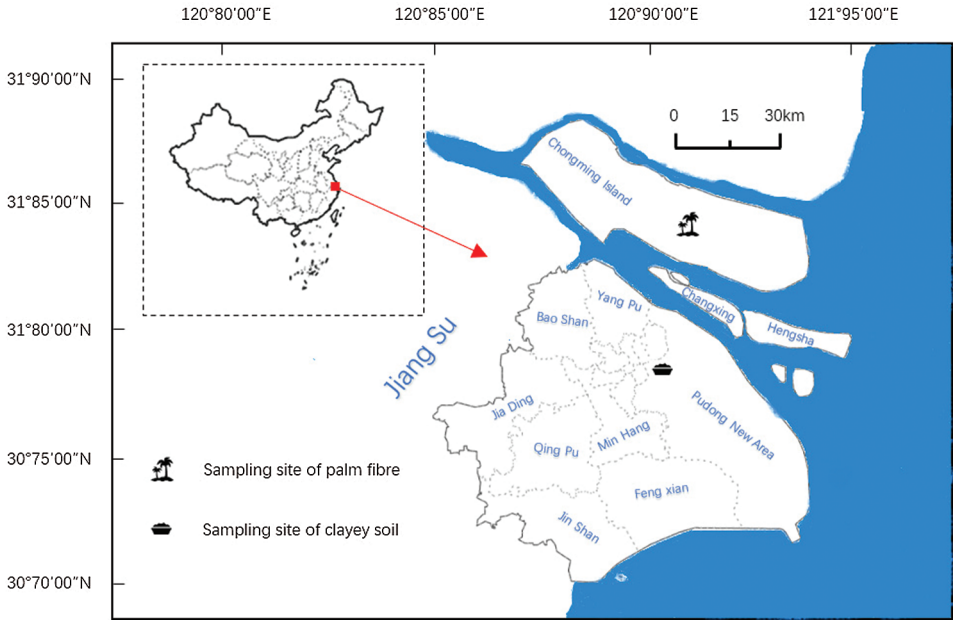

Figure 1: Geographic sites for collecting of palm fiber and soil

Table 1: Properties of palm fiber*

Properties	Value
Average diameter	0.192~1.240 mm
Tensile strength	89~222 MPa
Relative density	1.24
Elastic modulus	0.44~1.90 GPa
Natural elongation	5.0~23.45%
Bending rebound rate (after 1 h)	≥50%
Hygroscopic equilibrium moisture regain	16.65%
Wet equilibrium moisture regain	23.83%
Hygroscopic hysteresis difference	7.2%
Degree of crystallization	37.92%
Fatty wax	3.77%
Hydrotrope	2.80%
Pectin	0.60%
Hemicellulose	20.60%
Lignin	44.07%
Cellulose	28.16%

Note: *Provided by Shanghai Yiying Information Consulting and Management Co., Ltd.

2.1.2 Clayey Soil

The clayey soil used in this investigation has been collected from a construction side of Zhangjiang hi-tech park located in Pudong new area of Shanghai China (Fig. 1). The gathered clayey soil was air-dried, pulverized and sieved through 2 mm sieve in the laboratory of University of Shanghai for Science and Technology (USST). The particle size distribution curve of the soil is shown in Fig. 2. The soil is classified as clay of low plasticity (CL) as per ASTM D2487. The compaction tests were carried out on the soil according to ASTM D698, and the optimum water content (OWC) and maximum dry density (MDD) are 21.72% and 16.5 kg/m^3, respectively. Tab. 2 shows general physical and mechanical characteristics of soil used in the study.

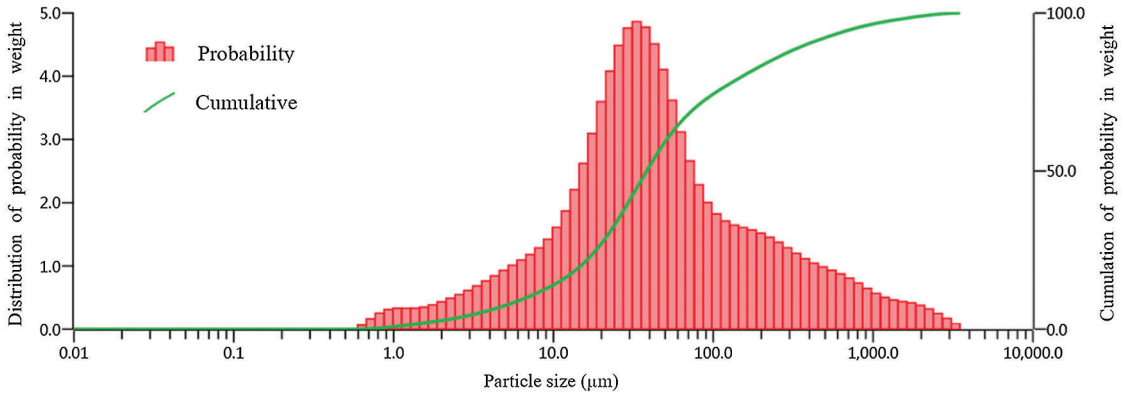

Figure 2: Particle size distribution of Shanghai clayey soil (analyzed by Laser Particle Sizer from Malvern Instruments Ltd., Shanghai)

Table 2: Physical and mechanical property of soil tested

Properties	Value
Optimum water content (OWC)	21.72
Liquid limit (W_L)	34.34
Plastic limit (W_P)	22.56
Plastic index (I_P)	11.78
Maximum dry unit density (MDD)	16.5 kN/m^3
Specific gravity (G_s)	2.73
Uniformity coefficient (c_u)	4.33
Coefficient of curvature (c_c)	1.97
Silt	57.5%
Clay	9.2%
Sand	33.3%

2.2 Methods

2.2.1 Specimen Preparation

Palm fibers brought back from the wildness are cleaned and air-dried, and then cut into fibers of 5, 10, 15 and 20 mm in lengths on a cutter for later use. Air-dried soil with specified weight is first blended with the required quantity of water, manually mixing for a proper period of time until a uniform state appears. Then the desired weight of cut-out palm fibers is added in small increments of 5 separate times manually. At least 3 minutes of manually mixing are required for each additional increment for the purpose of sample homogeneity. The mixing of palm fibers is done in a very careful way until a uniform mixture is observed by naked eyes. Then the soil mixture is put into polyethylene bag and kept in desiccators for 24 hours to ensure water balance. After above processing, the mixture is statically compacted in a cylindrical mold of 39 mm in inner diameter with detachable collars at both ends. For the purpose of above intention, the total quantity of moist soil-fiber mixture is put into the mold from one end after well installing the collar at the other end. The mixture is compacted inside the mold to produce specimens with sizes of 80 mm in height × 39 mm in diameter for unconfined compressive tests.

It should be noted that the fibers in the mixture tend to stick together and form lumps in the processing of the samples if 0.6% of palm fiber content is selected. Therefore, 0.6% of palm fiber is selected as the upper limit of the additives. Four palm fiber lengths of 5, 10, 15 and 20 mm and four fiber contents of 0.1, 0.2, 0.4 and 0.6% are selected to prepare the palm fiber-soil samples. Samples are prepared at the OWC-MDD compaction state according to the standard proctor compaction test. The details of testing scheme are presented in Tab. 3.

2.2.2 Scheme for Test and Analysis

The test series have different composition of two variables (Tab. 3). The two variables in the test are: length of palm fiber (5, 10, 15, 20 mm), content of palm fiber (0, 0.1, 0.2, 0.4, 0.6%), with samples always kept at OWC and MDD state. The evaluation indexes are: Unconfined compressive strength (UCS), ductility ratio (DR), secant modulus (SM), energy absorption capacity (EAC), failure pattern (FP). The UCS tests are conducted according to ASTM D2166/D2166M (ASTM 2013) at axial strain rate of 2.3 mm/min. Three parallel samples are prepared and tested for each set of parameters and the average is used to analyze their parameters for the purpose of the repeatability of the test results (Fig. 3). Together with the control samples, the total number of 51 samples are tested in this investigation. The flowchart for test and analysis is shown in Fig. 3.

Table 3: Test composition of unconfined compression test

No.	Water content (%)	Dry density (kN/m^3)	Fiber length (mm)	Fiber content (%)
1	21.72	16.5	0	0
2	21.72	16.5	5	0.1
3	21.72	16.5	10	0.1
4	21.72	16.5	15	0.1
5	21.72	16.5	20	0.1
6	21.72	16.5	5	0.2
7	21.72	16.5	10	0.2
8	21.72	16.5	15	0.2
9	21.72	16.5	20	0.2
10	21.72	16.5	5	0.4
11	21.72	16.5	10	0.4
12	21.72	16.5	15	0.4
13	21.72	16.5	20	0.4
14	21.72	16.5	5	0.6
15	21.72	16.5	10	0.6
16	21.72	16.5	15	0.6
17	21.72	16.5	20	0.6

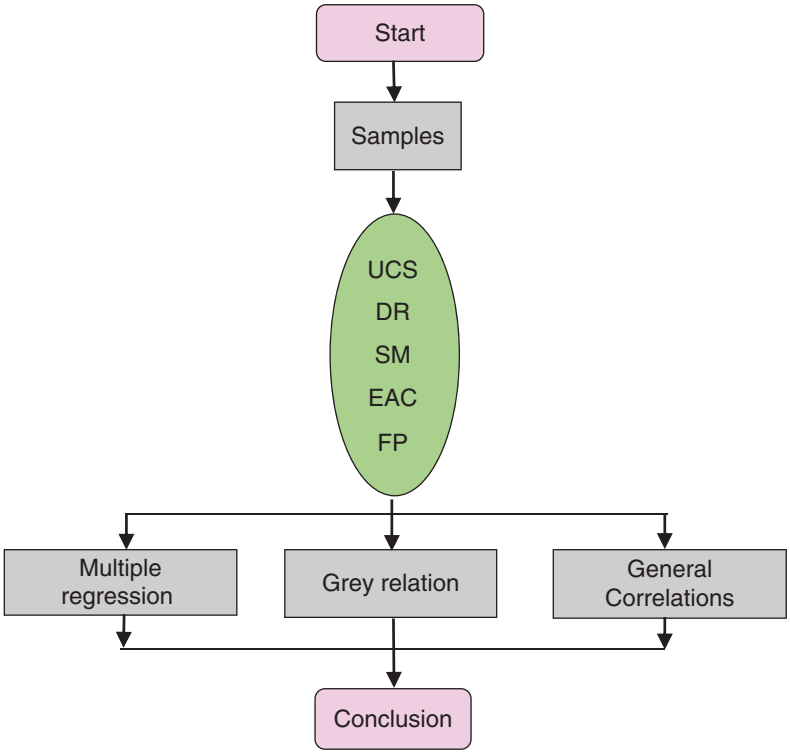

Figure 3: Flowchart for the test and analysis

After the testing results are obtained, the relationship between two variables (palm fiber content and length) and the five performance indexes (UCS, DR, SM, EAC, FP) is diagrammatically analyzed and assessed, respectively. Thereafter, the multiple regression, grey relation and general correlation relationship analysis are carried out to assess their relationships mathematically and quantitatively for the purpose of predicting the performance of reinforced soil more conveniently, cost-effectively and accurately as much as possible without the need of re-testing them in a specific scenario. Therefore this work is very meaningful in practice.

3 Results

3.1 Strength Characteristics

Fig. 4 shows the stress-strain curves of samples for different palm fiber contents at OWC and MDD as fiber length = 15 mm. For saving space, the results for other composition have not been presented. It can be seen from the Fig. 4 that the peak stresses are significantly increased for reinforced samples compared with unreinforced one and it increases with the content of palm fiber until fc = 0.4%. Thereafter, it decreases. This result suggests that there is maximum point of axial stress for the content of palm fiber that is around 0.4%. Sudden drop can be seen after peak stress for unreinforced sample (control), which indicates a nature of brittle deformation. But with the adding of palm fiber, it turns into gradual deformation, with increased failure strain accompanied by post-peak strength loss. The peak stress of sample with content of 0.4% and 15 mm in length is increased by approximately 80% compared with no-reinforced sample, with corresponding failure strain increased by about 146%.

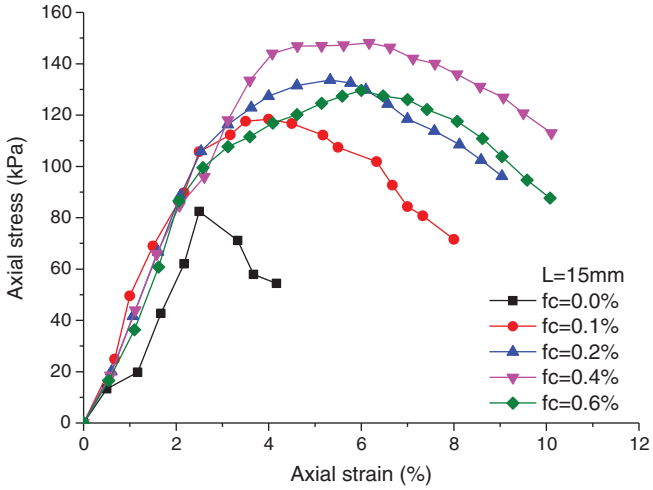

Figure 4: Relationship between stress and strain of samples for different palm fiber contents at OWC and MDD as fiber length = 15 mm

Fig. 5 shows the tress-strain curves of samples for different palm fiber lengths at OWC and MDD as palm fiber content Fc = 0.4%. It can be seen that peak stresses generally increase with the increase of palm fiber length, but when length = 15 mm, the peak stress is maximized, where the increase rate is approximately 80% compared to that of unreinforced samples. The failure axial strains are also significantly increased compared to that of unreinforced samples. For L = 15 mm, the increase rate of failure axial strain is approximately 146% compared to control samples. However, the peak stress and the corresponding failure strain for reinforced samples are increased gradually with the increase in fiber length. The test results show that as the content and length of palm fiber are 0.4% and 15 mm in length,

respectively, the peak strength is arrived with largest ductility. Fig. 6 shows the relationship between UCS and palm fiber content under different lengths.

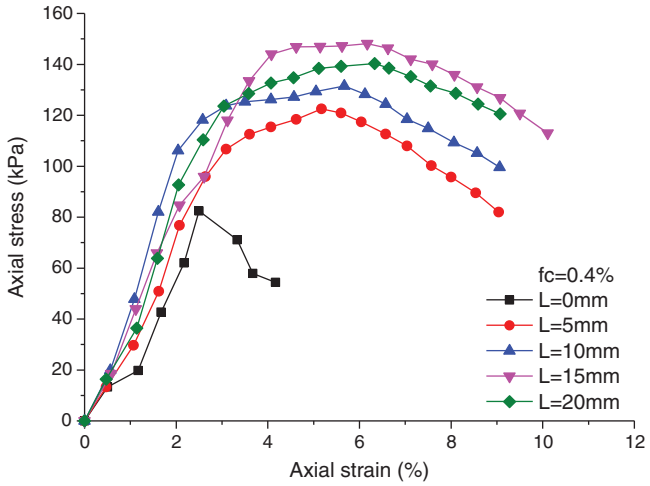

Figure 5: Relationship between stress and strain of samples for different palm fiber lengths at OWC and MDD as Fc = 0.4%

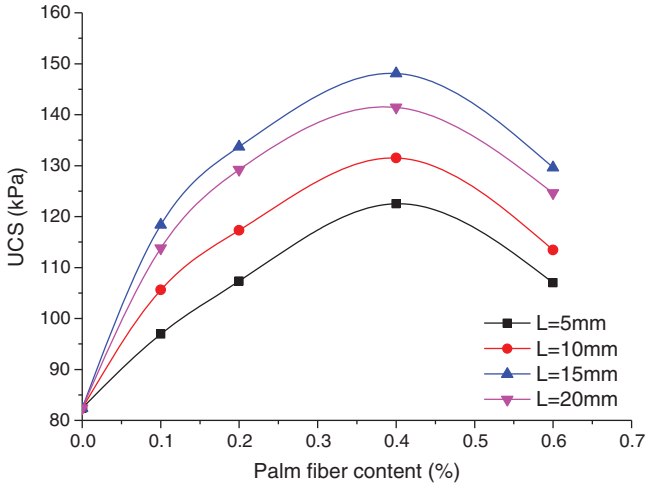

Figure 6: Change of UCS with palm fiber content under different lengths

3.2 Deformation Features

If ductility rate of a composite material is defined as DR = (failure strain of reinforced sample)/(failure strain of unreinforced sample), the DR of samples with different content and length of palm fiber can be calculated and plotted in Fig. 7. The variation of ductility rate is a little different from that of strength. It increases with the palm fiber content, and gradually declines after the 0.4% of content. But ductility rate increases with the length of palm fiber all the time without a turning point. This may be closely related to interaction mechanism of palm fiber with the surface of the soil particles. The increase in ductility rate decreases the nature of brittle failure of the soil, which is helpful to geotechnical structure and buildings in some specific conditions, because there will be more warning time for geotechnical engineers to remove the risks in some scenarios.

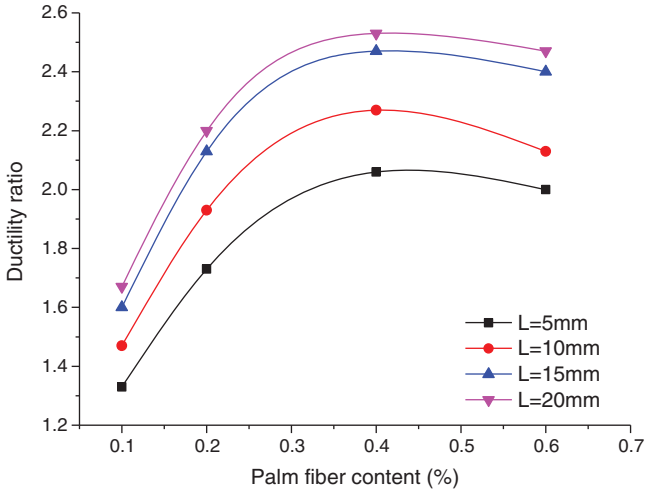

Figure 7: Curve between ductility ratio and palm fiber content under different lengths

3.3 Secant Modulus

The stiffness of the soil can be represented by the secant modulus, which is defined as the ratio of peak strength to failure strain. Fig. 8 shows the relationship between secant modulus and palm fiber content under different lengths. It can be observed that the secant modulus is decreased on the whole with the increase of both palm fiber content and length. With regard to the length, it seems to be a little different from that of content. There may be maximum points when L = 15 mm for different palm fiber contents. For L = 15 mm, the secant modulus decreases by about 34% as the fiber content is increased from 0 to 0.6%. Other related variations of indexes for samples tested are shown in Tab. 4. The increases in strength are accompanied by the decreases in stiffness, which also means the decrease in probability of brittle failure. It is of huge importance in some geotechnical engineering projects, especially in slope engineering, shallow foundation engineering, etc.

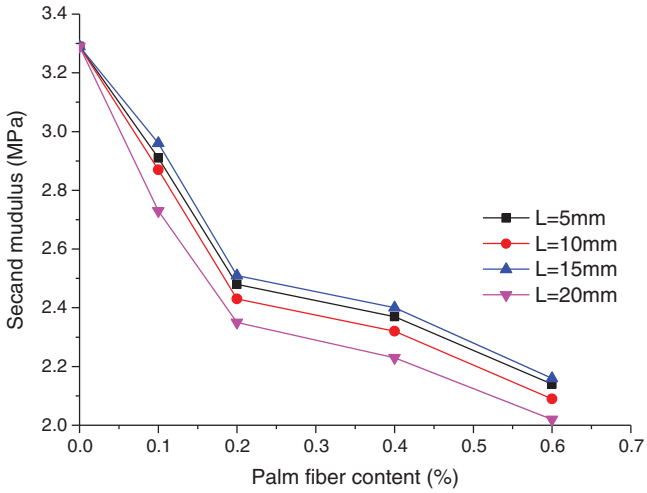

Figure 8: Change of secant modulus with palm fiber content under different lengths

Table 4: Summary of test results for specimens compacted at MDD and OWC

fc (%)	Fiber length (mm)	UCS (kPa)	Standard deviation (±kPa)	AV. Failure strain (%)	DR	EAC (kJ/m^3)	SM (MPa)
0	0	82.4	2.1	2.50	–	89.52	3.29
0.1	5	96.9	2.4	3.33	1.33	196.71	2.91
0.1	10	105.6	2.2	3.67	1.47	236.60	2.87
0.1	15	118.4	3.4	4.00	1.60	313.88	2.96
0.1	20	113.8	2.7	4.17	1.67	286.67	2.73
0.2	5	107.3	1.8	4.33	1.73	281.49	2.48
0.2	10	117.3	2.2	4.83	1.93	391.27	2.43
0.2	15	133.7	3.1	5.33	2.13	443.88	2.51
0.2	20	129.2	3.6	5.50	2.20	418.75	2.35
0.4	5	122.5	2.3	5.17	2.06	309.40	2.37
0.4	10	131.5	4.2	5.67	2.27	535.89	2.32
0.4	15	148.1	3.6	6.17	2.47	609.79	2.40
0.4	20	141.4	5.3	6.33	2.53	593.51	2.23
0.6	5	107.0	3.2	5.00	2.00	354.27	2.14
0.6	10	113.4	4.7	5.33	2.13	547.36	2.09
0.6	15	129.6	2.4	6.00	2.40	536.33	2.16
0.6	20	124.6	3.5	6.17	2.47	497.81	2.02

3.4 Energy Adsorption Capacity

The energy absorption capacity (EAC) is typically considered as another index indicating the characteristics of soil. It is generally defined as the area under stress–strain curves up to failure axial strain. In the present experiments, the increase in EAC approximately means the increase in peak strength or failure strain. Fig. 9 shows the relationship between energy adsorption capacity and palm fiber content under different lengths. It can be noted that EACs are generally increased with palm fiber contents until fc = 0.4%, thereafter declining, which suggests that 0.4% of palm fiber content may be a critical point for treated samples. The EAC also similarly sees increase with length of fiber until L = 15 mm. Therefore, for the present tests, fc = 0.4% and L = 15 mm may be the optimum selection for strengthening the soft soil, in which the EAC is increased by almost 580% compared to unreinforced sample. EACs are actually works done by axial stress in the tests, which equals numerically to the product of the axial stress multiplied by the distance it moves in the direction of axial stress. Therefore the larger the EAC, the higher the peak strength or failure strain in general. So EAC can be used as a proxy of strength or strain to some degree in some special conditions.

3.5 Failure Pattern

As a whole, the failure patterns are heavily influenced by the fiber content and length. With the increase in fiber content and length, the failure pattern changes gradually from brittle to ductile. This feature is embodied in appearance of samples. For saving space, the appearances of samples with only L = 15 mm and fc = 0, 0.1, 0.2, 0.4, 0.6%, respectively are selected as shown in Fig. 10. It can be observed that different failure patterns developed in samples of different fiber contents during and after the experiments. Double shear planes develop diagonally from the top and bottom along the longitudinal direction of

samples at initial strain during loading for unreinforced samples. Then they join together to form a predominant inclined shear plane at failure showing a brittle nature (a). With the increase of fiber content, in contrast, the failure pattern changes gradually from brittle to ductile. For samples with fc = 0.1 and 0.2%, there appear multiple small cracks on barreling on some parts of samples, indicating a transition from brittle to ductile (b, c). At higher fiber contents of 0.4 and 0.6%, there is a trend, though inconspicuously maybe due to the relatively small strain range, that there appears a slight bulging on the middle part of the samples with many fissures (d, e). All above phenomena may be explained by friction action between soil particle surface and fibers, and the bridging effect of fibers, which restrict the development of shear planes and the deformation of samples as the external force is applied.

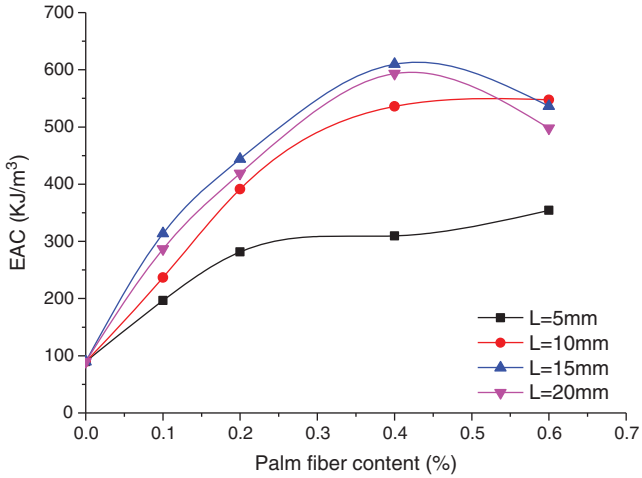

Figure 9: Change of energy adsorption capacity with palm fiber content under different lengths

(a) (b) (c) (d) (e)

Figure 10: Impact of palm fiber content on failure patterns at OWC and MDD as L = 15 mm of fiber length: (a) fc = 0, (b) fc = 0.1%, (c) fc = 0.2%, (d) fc = 0.4%, (e) fc = 0.6%

4 Mathematical Model

4.1 Multiple Regression Analysis

For analyzing the effect of the content and length of palm fiber on the performance indexes of Shanghai clayey soil reinforced with palm fiber more accurately and in detail, the statistical technique is applied to study their mathematical model. Fig. 11 shows the 3D fitting result, showing the variation of UCS with the content and length of palm fiber, from multiple regression analysis. It can be clearly observed that the UCS increases with the increase in content and length, but there is a maximum point which is achieved as fc = 0.4% and L = 15 mm. The neighboring points around the zenith are all below it in values. On the whole, it seems like a dome-shaped surface. The inset shows the regression parameters. The coefficient of determination (R^2) is about 0.93, showing a very good fitting. In regression, the fiber content and fiber length are designated as x, and y, respectively. Figs. 12 and 14 shows 3D fitting diagrams for the variation of ductility rate and energy adsorption capacity with content and length of palm fiber, respectively. They have the comparable change patterns with that of UCS, with determination coefficients of >0.90, showing a good fitting result. However, for secant modulus, there is a completely different variation pattern. The secant modulus decreases all the time with the increase in fiber content, but there is a maximum point of the secant modulus for the change in fiber length. That is, the secant modulus increases with the fiber length until L = 15 mm. Fig. 13 clearly shows the variations, with a determination coefficient slightly less than 0.9, still a good fitting. In order to more clearly present the formulas and parameters in Figs. 11–14, Tab. 5 has been made for this purpose.

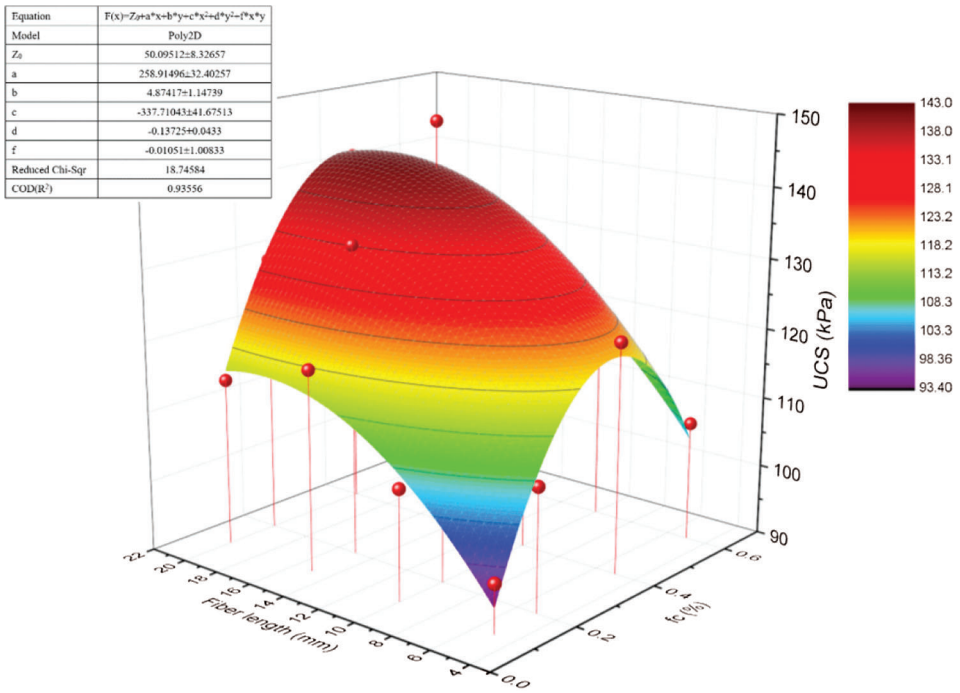

Figure 11: 3D fitting surface chart for effect of palm fiber content and length on UCS

4.2 Grey Relational Analysis

Grey relational analysis (GRA) refers to a method used to quantitatively describe and compare a system development and changing situation. Its basic idea is to determine whether the reference data series and several comparison data series are closely related by ascertaining their geometric similarity, which reflects the correlation degree between curves. In a nutshell, it is a statistical approach for determining which

variable(s) among a set of driving factors will more heavily impact the dependent variable. In this section, grey relational analysis is used to determine which one from fiber length and content will have more influence on the performance indexes of soil: namely, UCS, DR, SM, EAC. The grey relational degrees for UCS with content and length are calculated separately one by one following the calculation steps required by grey relational theory based on the testing data. And so do with the DR, SM, and EAC. The software embedded in Microsoft Excel has been used to finish above calculating work. The simple comparison criterion is followed, namely, the higher the grey relational degree the more important the driving force from content and length. For saving space, the specific formulae for computing have not been presented here. Tab. 6 shows the grey relational degrees of the performance indexes for reinforced soil with content and length of palm fiber. It can be seen from the Tab. 6 that the length of the palm fiber has higher degree of association than content except for EAC, indicating that in most cases the length of palm fiber may be a heavier driving force for the variation of soil characteristics. Due to the slight difference with degree of association for the length (0.60–0.72) and the content (0.49–0.70) of palm fiber, the magnitude of influence on performance is only relative.

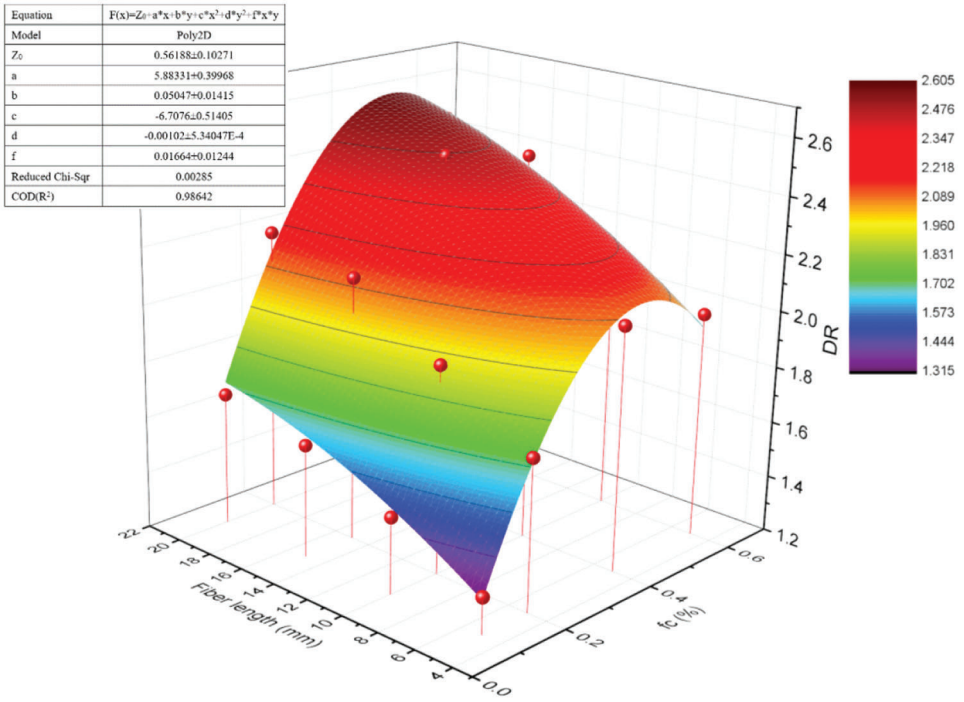

Figure 12: 3D fitting surface chart for effect of palm fiber content and length on DR

4.3 General Correlation Relationship Analysis

For further depicting the relationship among different performance indexes, the pairwise correlation coefficient is calculated based on the present testing data as shown in Tab. 7. The software used in the computational processes is also from the function in Microsoft Excel. The pairwise correlation coefficient among them are determined one by one. For saving space, the specific steps and computational formulae used have not been presented. It can be observed that the UCS is positively correlated with DR (R = 0.84) and EAC (R = 0.82), negatively correlated with SM (R = −0.41). DR is negatively correlated with SM (R = −0.84) and positively correlated with EAC (R = 0.92). SM is negatively correlated with EAC (R = −0.72). The pairwise correlation coefficient among the performance indexes of reinforced soil is very important in the survey and design of practical geotechnical engineering projects because one index can be approximately predicted from the other without the need of the laboratory or field experiment, saving in time and cost.

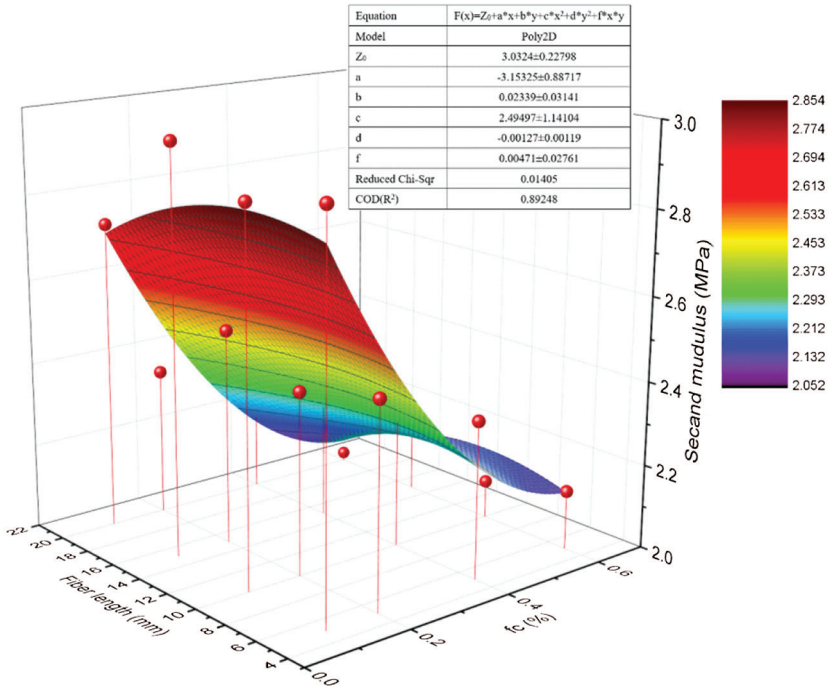

Figure 13: 3D fitting surface chart for effect of palm fiber content and length on SM

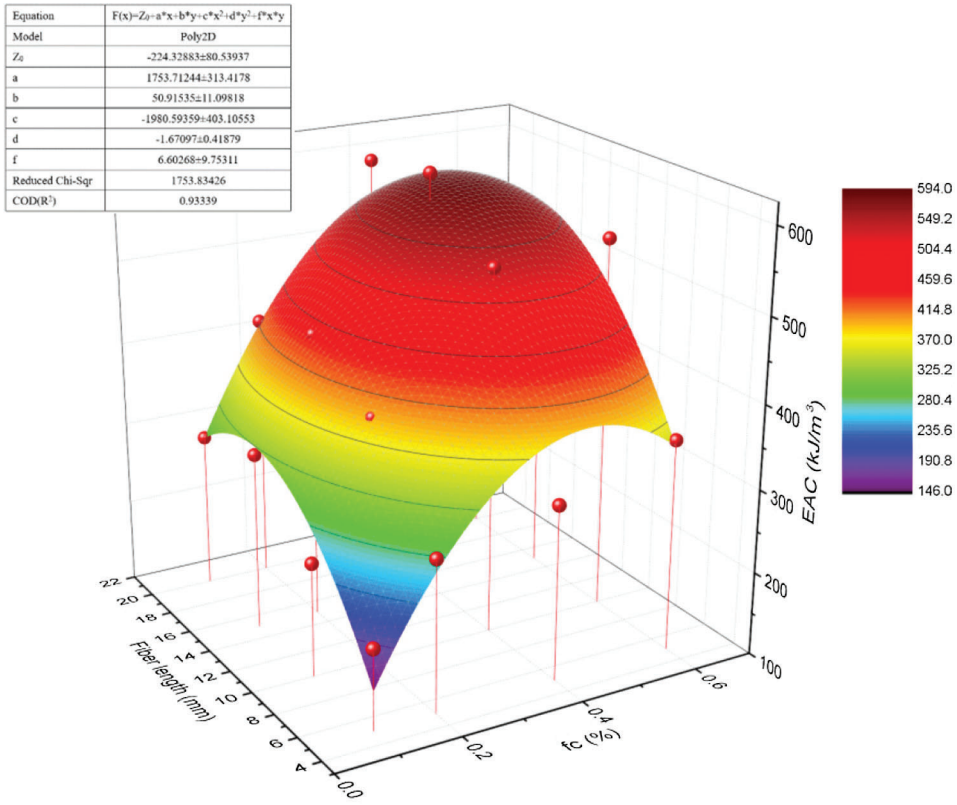

Figure 14: 3D fitting surface chart for effect of palm fiber content and length on EAC

Table 5: Summary of parameters for Figs. 11–14 with mathematic model of $F(x) = Z_0 + a*x + b*y + c*x^2 + d*y^2 + f*x*y$

	Z_0	a	b	c	d	f	Reduced C–S	R^2
UCS	50.09512 ± 8.32657	258.91496 ± 32.40257	4.87417 ± 1.14739	−337.71043 ± 41.67513	−0.13725 ± 0.0433	−0.01051 ± 1.00833	18.74584	0.93556
DR	0.56188 ± 0.10271	5.88331 ± 0.39968	0.05047 ± 0.01415	−6.7076 ± 0.51405	−0.00102 ± 5.3404	0.01664 ± 0.01244	0.00285	0.98642
SM	3.0324 ± 0.22798	−3.15325 ± 0.88717	0.02339 ± 0.03141	0.49497 ± 1.14104	−0.00127 ± 0.00119	0.00471 ± 0.02761	0.01405	0.89248
EAC	−224.32883 ± 80.53937	1753.71224 ± 313.4178	50.91535 ± 11.09818	−1980.59359 ± 403.10553	−1.67097 ± 0.41879	6.60268 ± 9.75311	1753.83426	0.93339

Table 6: Grey relational degree for performance indexes of treated soil

	UCS	DR	SM	EAC
Length	0.647	0.628	0.613	0.711
Content	0.560	0.579	0.490	0.676

Table 7: General correlation relationships among indices of soil tested

Indicator	UCS	DR	SM	EAC
UCS	–	0.84	−0.41	0.82
DR		–	−0.84	0.92
SM			–	−0.72
EAC				–

5 Discussions

For every set of samples, the test is repeated three times for the purpose of reproducibility of result. Although the total number of samples test is relatively small ($3 \times 17 = 51$), rigorous and careful preparation and implementation of all the experiments ensure the correctness and trustfulness of the result. And it adds to several statistical analysis of the test data. All the above efforts are expected to make up for the defect of small amount of samples, which also justify the analytic quality of this paper. In this paper, only the unconfined compressive test was carried out due to taking into consideration of workload of the paper. Direct shear test and triaxial shear test will be expected to consider in the future study in view of the equal importance of shear strength as UCS in practical engineering design and construction.

Microscopically, the action of the palm fiber in performance indexes on clayey soil can be mainly attributed to two functions: The friction action between fiber and soil surface, and the bridging action as tensile force is applied in soil body. The friction action can make the soil particles cement together more tightly, while the bridging action is able to resist against tensile stress. Fig. 15a shows the action mechanism for reinforced soil with fittest fiber content. The existence of fiber junction points can restrain the deformation of soil body as a whole. Therefore, the random inclusion of palm fibers into soil can change the total performance characteristics to a considerable degree. However, as excessive palm fibers are added, the performance of soil may be in most part adversely affected. Fig. 15b shows the action

mechanism for excessive palm fibers added. As excessive palm fibers are included, the close contact among the fibers can form a fiber partition surface in some parts of the soil body, which can cause the decrease of soil strength due to the fiber nature of more flexible than soil. This mechanism can fully explain why there is a maximum point in strength performance with the increase in content and length of palm fiber. In this study, 0.4% of palm fiber content and 15 mm in length are critical point, below which the strength performance will be enhanced while above which it will be weakened.

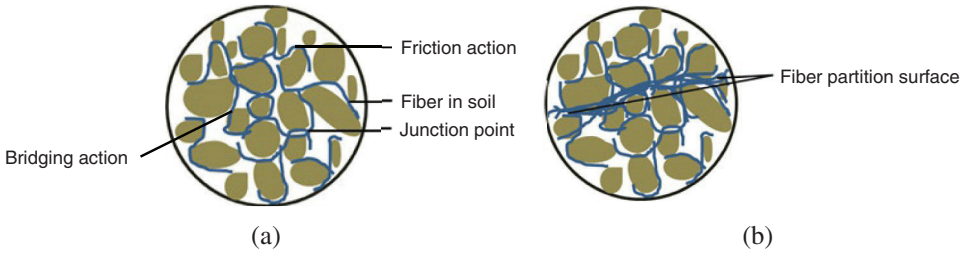

Figure 15: Mechanism analysis of palm fiber reinforced soil. (a) Action mechanism schematic for reinforced soil with fittest palm fiber content (b) Action mechanism schematic for excessive palm fibers added

For the purpose of comparison on how different fibers affect the soil reinforcement, Tab. 8 presents the results for reinforcing similar softy clay with different fibers. The titles of the table denote the researcher, reinforcement type, increase rate in UCS, optimum content and length of fibers, and soil type from left hand side to right hand side. And the result of the present study is shown in first row.

Table 8: comparison between current study and other related researches

Researchers	Additives	Increasing rate of UCS (%)	Optimum content (%)	Optimum length (mm)	Soil type
Present study	Palm fiber	80%	0.4	15	Clay
Jiang et al. [42].	Glass fiber	34%	0.1	9	Clay
Akbulut et al. [43].	Tire rubber fiber	92%	2	10	Clay
Akbulut et al. [43].	Polyethylene fiber	61%	0.2	15	Clay
Gao et al. [44].	Basalt fiber	31%	0.25	12	Clay
Wu et al. [45].	Sisal fiber	47%	0.4	5	Clay
Ramkrishnan et al. [46].	Jute fiber	84%	0.75	10	Clay

6 Conclusion

In this study, the unconfined compressive tests have been carried out on typical Shanghai clayey soil reinforced with local palm fibers, which is considered to be able to easily accessible, with different length and content. The performance indexes (UCS, DR, SM, EAC, FP) of reinforced soil, which are most commonly used in the geotechnical survey, design and construction in local civil engineering projects, are considered as assessment targets. The major conclusions drawn from the current investigation can be summarized as follows:

1. Overall, the palm fiber has a positive impact on soft soil. The unconfined compressive strength of Shanghai clayey soil reinforced with local pam fiber increases with the content and length of fiber until a critical point appearing (fc = 0.4%, L = 15 mm).

2. The ductility of reinforced soil is significantly increased with the content and length of palm fiber. The ductility rate (DR) is 2.47 with samples at fc = 0.4% and L = 15 mm. on the contrary, the secant modulus of reinforced soil is considerably decreased with content and length of palm fiber as a whole, which is decreased by 34% with samples at fc = 0.6% and L = 15 mm compared with the unreinforced soil.
3. The energy adsorption capacity is generally increased with the content and length of palm fiber, which is increased by 580% for samples with fc = 0.4% and L = 15 mm compared to unreinforced soil.
4. The failure pattern trend is generally transitioned from brittle failure to ductile failure, which appears in the shape from one single diagonal shear plane, multiple fissures to bulging in the middle of the samples, indicating the increase of the ductility after reinforcement.
5. The mathematic model has been established to further depict their detailed, accurate and quantitative relationship. The grey relational analysis has been applied to analyze the test result to obtain the slightly more predominance of length influence than content of palm fiber. It comes on top of the general correlation pairwise analysis, all of which are of huge importance in practical engineering, because it can provide the fundamental reference data for geotechnical investigation, design, construction and maintenance in the context of emphasizing the environmental protection, sustainable development and resisting against climate change. The range of content and length variables, if referenced in practical engineering, should be considered in the vicinity of laboratory results, which will save considerably both in time and economy, compared to additional large-scale field test.

Acknowledgement: The authors will first of all thank Andrian Batugin for the overall idea of the paper, Ekin Koken for the specific engineering properties of the reinfornced soil, Cristea Lavinia for work of statistics and regression of testing result, Baoshi Liu for collection of soil tested and Xiaoru Huang for collection of palm fiber.

Funding Statement: The authors will also thank Shanghai municipal government for financial support (No. 57-19-119-002).

Conflicts of Interest: The authors declare that they have no conflicts of interest to report regarding the present study.

References

1. Prabakar, J., Sridhar, R. S. (2002). Effect of random inclusion of sisal fibre on strength behaviour of soil. *Construction and Building Materials, 16(2),* 123–131. DOI 10.1016/S0950-0618(02)00008-9.
2. Islam, M. T., Chittoori, B. C. S., Burbank, M. (2020). Evaluating the applicability of biostimulated calcium carbonate precipitation to stabilize clayey soil. *Journal of Materials in Civil Engineering, 32(3),* 04019369. DOI 10.1061/(ASCE)MT.1943-5533.0003036.
3. Anagnostopoulos, C. A., Papalianga, T. T., Konstantinidis, D., Patronis, C. (2013). Shear strength of sands reinforced with polypropylene fibers. *Geotechnical and Geological Engineering, 31(2),* 401–423. DOI 10.1007/s10706-012-9593-3.
4. Qu, J. L., Zhu, H. (2020). Modifying mechanical properties of Shanghai clayey soil with construction waste and pulverized lime. *Science and Engineering of Composite Materials, 27(1),* 163–176. DOI 10.1515/secm-2020-0016.
5. Sharma, R. K., Hymavathi, J. (2016). Effect of fly ash, construction demolition waste and lime on geotechnical characteristics of a clayey soil: A comparative study. *Environmental Earth Sciences, 75(5),* 377. DOI 10.1007/s12665-015-4796-6.
6. Onyrlowe, K. C. (2019). Review on the role of solid waste materials in soft soils reengineering. *Materials Science for Energy Technologies, 2(1),* 46–51. DOI 10.1016/j.mset.2018.10.004.

7. Cheng, Y. Z., Wang, S., Li, J., Huang, X. M., Li, C. et al. (2018). Engineering and mineralogical properties of stabilized expansive soil compositing lime and natural pozzolans. *Construction and Building Materials, 187,* 1031–1038. DOI 10.1016/j.conbuildmat.2018.08.061.
8. Wang, Z. S., Wang, L. J., Cui, Z. L., Zhou, M. (2011). Effect of recycled coarse aggregate on concrete compressive strength. *Transactions of Tianjin University, 17(3),* 229–234. DOI 10.1007/s12209-011-1499-2.
9. Pachauri, S., Priya, M. I., Garg, A. (2016). Comparative analysis of strength characteristics of soil reinforced with coir and polypropylene fibers. *Ground Improvement Techniques and Geosynthetics, IGC 2016, 2,* 355–362. DOI 10.1007/978-981-13-0559-7_40.
10. Wang, Y. X., Guo, P. P., Shan, S. B., Yuan, H. P., Yuan, B. X. (2016). Study on strength influence mechanism of fiber-reinforced expansive soil using jute. *Geotechnical and Geological Engineering, 34(4),* 1079–1088. DOI 10.1007/s10706-016-0028-4.
11. Krishna Rao, S. V., Nasr, A. M. A. (2012). Laboratory study on the relative performance of silty-sand soils reinforced with linen fiber. *Geotechnical and Geological Engineering, 30(1),* 63–74. DOI 10.1007/s10706-011-9449-2.
12. Gherisl, A., Hamrounil, A. (2020). Treatment of an expansive soil using vegetable (DISS) fibre. *Innovative Infrastructure Solutions, 5(1),* 30. DOI 10.1007/s41062-020-0281-5.
13. Momoh, E. O., Osofero, A. I. (2020). Recent developments in the application of oil palm fibers in cement composites. *Frontiers of Structural and Civil Engineering, 14(1),* 94–108. DOI 10.1007/s11709-019-0576-9.
14. Chen, C., Zhang, G., Zornberg, J. G., Morsy, A. M., Huang, J. (2020). Interface bond behavior of tensioned glass fiber-reinforced polymer (GFRP) tendons embedded in cemented soils. *Construction and Building Materials, 263 (10),* 120–132. DOI 10.1016/j.conbuildmat.2020.120132.
15. Yamashita, E., Cikmit, A. A., Tsuchida, T., Hashimoto, R. (2020). Strength estimation of cement-treated marine clay with wide ranges of sand and initial water contents. *Soils and Foundations, 60(5),* 1065–1083. DOI 10.1016/j.sandf.2020.05.002.
16. Long, G. C., Li, L. H., Li, W. G., Ma, K. L., Dong, W. K. et al. (2019). Enhanced mechanical properties and durability of coal gangue reinforced cement-soil mixture for foundation treatments. *Journal of Cleaner Production, 231(10),* 468–482. DOI 10.1016/j.jclepro.2019.05.210.
17. Liu, C., Lv, Y., Yu, X. J., Wu, X. (2020). Effects of freeze-thaw cycles on the unconfined compressive strength of straw fiber−reinforced soil. *Geotextiles and Geomembranes, 48(4),* 581–590. DOI 10.1016/j.geotexmem.2020.03.004.
18. Tang, C. S., Cheng, Q., Wang, P., Wang, H. S., Wang, Y. et al. (2020). Hydro-mechanical behavior of fiber reinforced dredged sludge. *Engineering Geology, 276,* 105779. DOI 10.1016/j.enggeo.2020.105779.
19. Asim, M., Uddin, G. M., Jamshaid, H., Raza, A., Tahir, Z. U. R. et al. (2020). Comparative experimental investigation of natural fibers reinforced light weight concrete as thermally efficient building materials. *Journal of Building Engineering, 31,* 101411. DOI 10.1016/j.jobe.2020.101411.
20. Ardanuy, M., Claramunt, J., Toledo Filho, R. D. (2015). Cellulosic fiber reinforced cement-based composites: A review of recent research. *Construction and Building Materials, 79,* 115–128. DOI 10.1016/j.conbuildmat.2015.01.035.
21. Ramakrishna, G., Sundararajan, T. (2005). Impact strength of a few natural fibre reinforced cement mortar slabs: A comparative study. *Cement and Concrete Composites, 27(5),* 547–553. DOI 10.1016/j.cemconcomp.2004.09.006.
22. Colorado, H. A., Loaiza, A. (2018). Portland cement paste blended with pulverized coconut fibers. *Advances in Materials Science for Environmental and Energy Technologies, 6(Suppl 2),* 77–84. DOI 10.1002/9781119423799.ch8.
23. Elenga, R. G., Dirras, G. F., Goma, M. J., Djemia, P., Biget, M. P. (2009). On the microstructure and physical properties of untreated raffia textilis fiber. *Composites. Part A: Applied Science and Manufacturing, 40(4),* 418–422. DOI 10.1016/j.compositesa.2009.01.001.
24. Agarwal, A., Nanda, B., Maity, D. (2014). Experimental investigation on chemically treated bamboo reinforced concrete beams and columns. *Construction and Building Materials, 71,* 610–617. DOI 10.1016/j.conbuildmat.2014.09.011.

25. Asim, M., Abdan, K., Jawaid, M., Nasir, M., Dashtizadeh, Z. et al. (2015). A review on pineapple leaves fibre and its composites. *International Journal of Polymer Science, 2015(6),* 1–16. DOI 10.1155/2015/950567.
26. Oladele, I. O., Omotoyinbo, J. A., Adewara, J. O. T. (2010). Investigating the effect of chemical treatment on the constituents and tensile properties of sisal fibre. *Journal of Materials and Minerals Characterization and Engineering, 9(6),* 569–582. DOI 10.4236/jmmce.2010.96041.
27. Agopyan, A., Savastano, H. J. J., John, V. M., Cincotto, M. A. (2005). Developments on vegetable fibre-cement based materials in Sao Paulo, Brazil: An overview. *Cement and Concrete Composites, 27(5),* 527–536. DOI 10.1016/j.cemconcomp.2004.09.004.
28. Chan, C. M. (2011). Effect of natural fibres inclusion in clay bricks: Physicomechanical properties. *International Journal of Civil and Environmental Engineering, 5(1),* 7–13. DOI 10.5281/zenodo.1331783.
29. Sethunarayanan, R., Chockalingam, S., Ramanathan, R. (1989). Natural fiber reinforced concrete. *International Conference on Recent Developments in Concrete Fiber Composites*. *Transportation Research Board, Washington DC*, 1989,
30. Claramunt, J., Fernández-Carrasco, L. J., Ventura, H., Ardanuy, M. (2016). Natural fiber nonwoven reinforced cement composites as sustainable materials for building envelopes. *Construction and Building Materials, 115,* 230–239. DOI 10.1016/j.conbuildmat.2016.04.044.
31. Aziz, M. A., Paramasivam, P., Lee, S. L. (1981). Prospects for natural fibre reinforced concretes in construction. *International Journal of Cement Composites and Lightweight Concrete, 3(2),* 123–132. DOI 10.1016/0262-5075(81)90006-3.
32. Olaoye, R. A., Oluremi, J. R., Ajamu, S. O. (2013). The use of fibre waste as complement in concrete in concrete for a sustainable environment. *Innovative Systems Design and Engineering, 4(9),* 91–97.
33. Ismail, S., Yaacob, Z. (2011). Properties of laterite bricks reinforced with oil palm empty fruit bunch fibres. *Pertanika Journal of Science & Technology, 19(1),* 22–43.
34. Benmansour, N., Agoudjil, B., Gherabli, A., Kareche, A., Boudenne, A. (2014). Thermal and mechanical performance of natural mortar reinforced with date palm fibers for use as insulating materials in buildings. *Energy and Buildings, 81,* 98–104. DOI 10.1016/j.enbuild.2014.05.032.
35. Al-Oraimi, S. K., Seibi, A. C. (1995). Mechanical characterisation and impact behaviour of concrete reinforced with natural fibres. *Composite Structures, 32(1–4),* 165–171. DOI 10.1016/0263-8223(95)00043-7.
36. Zahra, N. F., Fayrouz, Z., Lamis, A., Mondher, Z. (2017). Mechanical performance of Doum Palm Fiber-Reinforced Plater Mortars. *Design and Modeling of Mechanical Systems—III, 2017,* 473–482. DOI 10.1007/978-3-319-66697-6.
37. Rashid, B., Leman, Z., Jawaid, M., Ghazali, M. J., Ishak, M. R. (2016). The mechanical performance of sugar palm fibres (Ijuk) reinforced phenolic composites. *International Journal of Precision Engineering and Manufacturing, 17(8),* 1001–1008. DOI 10.1007/s12541-016-0122-9.
38. Wu, G. C., Pan, S. H., Tang, G. L. (2006). Risk and quarantine measures of introducing palm fiber plants in Shanghai. *Plant Quarantine, (2),* 113–114.
39. Zhang, T. H., Li, X. L., Cheng, L., Mao, L. (2010). Properties abd application status of palm fiber. *Technical Textiles, 28(6),* 35–38.
40. Qu, J. L., Zhao, D. X. (2016). Stabilising the cohesive soil with palm fibre sheath strip. *Road Materials and Pavement Design, 17(1),* 87–103. DOI 10.1080/14680629.2015.1064010.
41. Yin, W. W., Chen, C. J., Shi, J. J., Wang, G. H. (2019). Research on the biodegradability of palm fiber. *Shanghai Wextile Science & Technology, 47(3),* 61–64. DOI 10.16549/j.cnki.issn.1001−2044.2019.03.020.
42. Jiang, Z. L., Wang, C. G., Xiao, W., Ruan, B. (2020). Laboratory investigation and numerical simulation of unconfined compressive strength of glass fiber reinforced soil. *Journal of Railway Science and Engineering, 17(6),* 1404–1410. DOI 10.19713/j.cnki.43-423/u.T20200074.
43. Akbulut, S., Arasan, S., Kalkan, E. (2007). Modification of clayey soils using scrap tire rubber and synthetic fibers. *Applied Clay Science, 38(1–2),* 23–32. DOI 10.1016/j.clay.2007.02.001.

44. Gao, L., Hu, G. H., Xu, N., Fu, J. Y., Xiang, C. et al. (2015). Experimental study on unconfined compressive strength of basalt fiber reinforced clay soil. *Advances in Materials Science and Engineering, 2015,* 1–8. DOI 10.1155/2015/561293.

45. Wu, Y. K., Niu, B., Sang, X. S. (2012). Experimental study of mechanical properties of soil randomly included with sisal fiber. *Hydrogeology & Engineering Geology, 39(6),* 77–81. DOI 10.16030/j.cnki.issn.1000-3665.2012.06.013.

46. Ramkrishnan, R., Karthik, V., Sruthy, M. R., Sharma, A. (2018). Soil reinforcement and slope stabilization using natural jute fibres. *New Solutions for Challenges in Applications of New Materials and Geotechnical Issues,* 130–143. DOI 10.1007/978-3-319-95744-9.

Appendix

The original test dada for unconfined compressive strength

No.	fc (%)	Fiber length (mm)	UCS (kPa)	AV. UCS (kPa)	Standard deviation (± kPa)	Failure strain (%)	AV. Failure strain (%)
1	0	0	82.89	82.41	2.09	2.5	2.50
2	0	0	84.21			2.5	
3	0	0	80.12			2.5	
4	0.1	5	97.68	96.94	2.43	3.5	3.33
5	0.1	5	94.23			3.0	
6	0.1	5	98.92			3.5	
7	0.1	10	105.58	105.60	2.23	3.5	3.67
8	0.1	10	107.84			4.0	
9	0.1	10	103.39			3.5	
10	0.1	15	121.83	118.37	3.38	4.5	4.00
11	0.1	15	118.21			4.0	
12	0.1	15	115.08			3.5	
13	0.1	20	110.97	113.76	2.73	4.0	4.17
14	0.1	20	116.43			4.5	
15	0.1	20	113.89			4.0	
16	0.2	5	105.51	107.28	1.79	4.0	4.33
17	0.2	5	109.08			4.5	
18	0.2	5	107.25			4.5	
19	0.2	10	114.81	117.31	2.17	4.5	4.83
20	0.2	10	118.68			5.0	
21	0.2	10	118.43			5.0	
22	0.2	15	133.18	133.69	3.11	5.5	5.33
23	0.2	15	137.03			5.5	
24	0.2	15	130.87			5.0	

(continued).

No.	fc (%)	Fiber length (mm)	UCS (kPa)	AV. UCS (kPa)	Standard deviation (± kPa)	Failure strain (%)	AV. Failure strain (%)
25	0.2	20	125.77	129.17	3.61	5.0	5.50
26	0.2	20	128.78			5.5	
27	0.2	20	132.96			6.0	
28	0.4	5	124.13	122.54	2.31	5.5	5.17
29	0.4	5	123.61			5.0	
30	0.4	5	119.89			5.0	
31	0.4	10	133.47	131.51	4.21	6.0	5.67
32	0.4	10	126.67			5.0	
33	0.4	10	134.38			6.0	
34	0.4	15	149.98	148.09	3.58	6.0	6.17
35	0.4	15	150.33			6.5	
36	0.4	15	143.97			6.0	
37	0.4	20	143.38	141.38	5.32	6.5	6.33
38	0.4	20	135.35			6.0	
39	0.4	20	145.42			6.5	
40	0.6	5	106.58	107.01	3.19	5.0	5.00
41	0.6	5	110.39			5.5	
42	0.6	5	104.05			4.5	
43	0.6	10	126.81	131.43	4.74	5.0	5.33
44	0.6	10	131.18			5.0	
45	0.6	10	136.29			6.0	
46	0.6	15	132.34	129.58	2.42	6.0	6.00
47	0.6	15	128.59			6.0	
48	0.6	15	127.82			6.0	
49	0.6	20	123.54	124.61	3.50	6.0	6.17
50	0.6	20	121.76			6.0	
51	0.6	20	128.52			6.5	